

## Unveiling The Patterns Of Cardiac Fibrosis Using 3d Radiomics In Heart Failure Patients

Indresh Yadav<sup>1</sup>, Majid.Ali<sup>2</sup>, Hayder A. H. Jalil<sup>3</sup>, Dr Avrina Kartika Ririe MD<sup>4</sup>, Dr. Jaisingh Rajput MD<sup>5</sup>, Noman Ullah Wazir<sup>6\*</sup>, Dimitrios Platis<sup>7</sup>, Mohammad Yassin<sup>8</sup>

<sup>1</sup>MBBS, Nuvance Health/ VBMC, Department of Internal Medicine, USA,

Email: [yadavindresh104@gmail.com](mailto:yadavindresh104@gmail.com)

<sup>2</sup>Medical Research Assistant, Department of Physiology, Faculty of Medicine University Technology Mara Sungai Buloh Campus Malaysia, Email: [hingorjomajid93@gmail.com](mailto:hingorjomajid93@gmail.com)

<sup>3</sup>Department of Pharmacology and Toxicology, College of Pharmacy, Al-Bayan University, Baghdad, Iraq, Email: [haiderhassan306@gmail.com](mailto:haiderhassan306@gmail.com)

<sup>4</sup>Brain & Heart Center Department, Mohammad Hoesin General Hospital, Palembang, Indonesia, Email: [avrinaririe@gmail.com](mailto:avrinaririe@gmail.com)

<sup>5</sup>Director of Stabler Clinic, Department of Family Medicine, Baptist Family Medicine Residency Program, State Alabama, US, Email: [1981jkr@gmail.com](mailto:1981jkr@gmail.com)

<sup>6\*</sup>Associate professor of Anatomy, Peshawar medical College,

Email: [dr.noman.wazir@gmail.com](mailto:dr.noman.wazir@gmail.com)

<sup>7</sup>Medical Doctor, School of Medicine, National and Kapodistrian University of Athens, Athens, Greece,

Email: [platisdim27@gmail.com](mailto:platisdim27@gmail.com)

<sup>8</sup>Medical Student (Med 4), Faculty of Medical Sciences, Lebanese University, Beirut, Lebanon, Email:

[Mohamad.kh.yassin@gmail.com](mailto:Mohamad.kh.yassin@gmail.com)

---

Cite this paper as: Indresh Yadav<sup>1</sup>, Majid.Ali, Hayder A. H. Jalil, Avrina Kartika Ririe MD, Jaisingh Rajput MD, Noman Ullah Wazir, Dimitrios Platis, Mohammad Yassin (2024) Unveiling The Patterns Of Cardiac Fibrosis Using 3d Radiomics In Heart Failure Patients *Frontiers in Health Informatics*, 13 (3), 4833-4840

---

### ABSTRACT:

**Background:** Myocardial perfusion imaging using <sup>99m</sup>Tc-MIBI SPECT is valuable for assessing chronic myocardial infarction (MI). However, conventional analysis may overlook heterogeneity within fixed perfusion deficits.

**Objective:** This study aims to utilize radiomics analysis to identify and characterize heterogeneity within fixed perfusion deficits caused by chronic MI.

**Methods:** A retrospective cohort study was conducted in a single-centre outpatient setting. Twenty-eight patients (9 women, 9 men; mean age 68 ± 11 years) with fixed perfusion abnormalities on resting polar map images and a history of chronic MI were included. Radiomics data were extracted using Mazda software from regions of interest within the homogeneous-uptake myocardium and fixed defects with probable heterogeneous uptake. Random Forest/LogitBoost algorithms in the WEKA artificial intelligence program were employed for analysis, achieving 100% sensitivity, specificity, and area under the ROC curve (AUC) for classifying heterogeneous vs. homogeneous textures. Heterogeneous textures derived from co-occurrence and run-length matrices were identified as significantly more predictive (AUC 100%) than homogeneous textures by binomial logistic regression analysis.

**Results:** Identified heterogeneous textures (e.g., 135dr\_ShrtREmp, 45dgr\_ShrtREmp, 45dgr\_Fraction, S(2,-2) InvDfMom, Horzl\_Fraction) demonstrated superior predictive capability for heterogeneity within fixed perfusion deficits compared to homogeneous textures.

**Conclusion:** Radiomics analysis enables the prediction and quantification of heterogeneity within permanent

*perfusion abnormalities. This approach offers potential future applications for myocardial perfusion SPECT in individuals with persistent myocardial infarction, thereby enhancing diagnostic and prognostic capabilities in this population.*

**KEYWORDS:** *SPECT myocardial perfusion using 99mTc-MIBI, radiomics, artificial intelligence, and chronic myocardial infarction.*

## INTRODUCTION:

Histopathology of chronic myocardial infarction (CMI) reveals fibrosis, myofibroblasts with scar tissue, and what seems to be a fixed perfusion deficit on resting SPECT myocardial perfusion (PMSG) imaging. A method called radiomics is used to extract several quantitative data points, or parameters, from a specific region of interest (ROI) in medical pictures. In nuclear cardiology, many characteristics that are crucial for diagnosis can be observed visually, such as the myocardium's hypo- or hyper uptake of radiotracers. However, other metrics that measure tissue components or heterogeneity are not visible to the naked eye. Radiomics is frequently utilized in oncology imaging to extract texture patterns that are clinically used in tumour diagnosis and to distinguish benign from malignant tumours (Zhao et al., 2021).

Radiomics has primarily focused on cardiomagnetic resonance imaging (CMRI) and computed tomography (C.T.) in patients with chronic myocardial infarction (CMI) to assess scar heterogeneity. Additionally, in nuclear cardiology, SPECT images of myocardial perfusion with or without C.T. have been studied to assess coronary artery calcification, myocardial ischemia, and in patients with cardiomyopathy who have heart failure. Our goal is to identify heterogeneity in the scar caused by chronic myocardial infarction and in the hypo uptake of MIBI due to fixed perfusion defects (D.F.) visible in resting SPECT myocardial perfusion polar maps. We will do this by applying radiometric concepts that are the same as those used in C.T. and CRMN and comparing them with textures extracted from remote myocardium with homogeneous MIBI uptake (Benfante et al., 2023).

## METHODOLOGY:

A single-centre observational study using 99m-Tc-sestamibi was carried out on 28 consecutive BMI outpatients who were referred to the Radioisotope Laboratory of Córdoba for the PMGS study between February 2021 and March 2023. The Institution's Ethics Committee approved the study protocol in compliance with the Declaration of Helsinki. As directed by the treating physician, myocardial perfusion with 99mTc-MIBI was carried out utilizing the one-day protocol, ergometric exercise, pharmacological challenge, or a combination of these, along with rest. Myocardial perfusion is regulated by 99mTc-MIBI using SPECT. The experiments were carried out following the guidelines endorsed by the European Association of Nuclear Medicine (EANM) and demonstrated. SPECT images were obtained in both the supine and prone positions following ergometric exercise regimes and pharmacological intervention with dipyridamole or its combination with exercise (Rdzanek et al.).

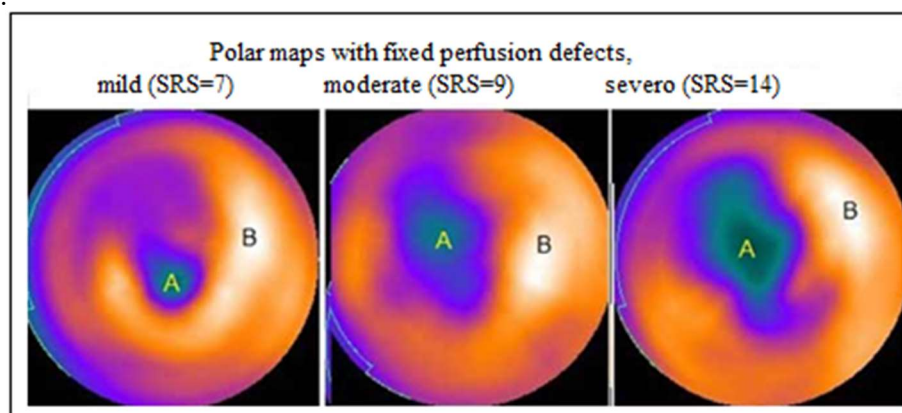


*Figure 1: myocardial perfusion is seen using 99mTc-MIBI. Areas of focus (ROI). In the corrected perfusion defect, radio mic images are retrieved using the Mazda program, whereas, in the remote non-infarcted myocardium, radio mic images are obtained.*

The study was conducted 15-30 minutes after intravenous administration of 99mTc-MIBI to address artefacts caused by diaphragmatic attenuation. The study was then performed at rest 4 hours later. The reconstruction, axis orientation, and viewing and quantification of polar maps were performed using a dual-detector gamma camera and the QPS program (Cedars-Sinai, Los Angeles, USA). The quantification of hypo uptake at rest, resulting from a fixed defect (F.D.) of perfusion, which is believed to be caused by necrosis resulting from chronic myocardial infarction, was performed using the Quantitative Perfusion Score (QPS). The rest score (SRS) was then categorized into three levels: a) mild SRS ranging from 4 to 7, b) moderate SRS ranging from 8 to 12, and c) severe SRS above 122 (Solanki et al., 2022).

**Radiomics**

The Mazda program (version 4.6, Institute of Electronics, Technical University of Lodz, Poland) was used to extract radiomics texture frames. This was done by manually drawing two regions of interest (ROI) on the polar map images. The ROI was then interpreted visually and quantitatively to determine the D.F. Additionally; the ROI was extracted in the remote myocardium with uniform uptake, where the radiomics texture images were obtained (Figure 1). The program employs a normalization technique to reduce the impact of contrast and brightness fluctuations within the intensity range of ( $\mu-3SD$ ,  $\mu+3SD$ ) in grayscale photographs. Two hundred seventy-nine distinct texture frames are retrieved from the ROIs collected in the previous stage. These frames are generated using grayscale pixel intensity differences, which are categorized into six statistical categories as defined by the author. The texture squares that were retrieved were classified into two groups: a) repaired defects and b) myocardium with uniform absorption (Noguera et al., 2022; uz Zaman, 2022).

The utilization of artificial intelligence for the extraction of texture frames. Texture analysis is a statistical methodology employed in the interpretation of medical images, which relies on the examination of pixel intensity distribution and its correlation with adjacent pixels. Artificial intelligence and radiomics have a reciprocal interaction. The primary rationale for employing artificial intelligence in radiomics is the need for analysis tools capable of handling vast quantities of data, in contrast to conventional statistical methods. Artificial intelligence is primarily utilized for the analysis of two- and three-dimensional (2D-3D) images through algorithms that learn from the data provided by radiomics. These algorithms then analyze the images and generate predictions, which are crucial for performing diagnostic classification (Lin & Dey, 2022).

**TABLE 1: Current myocardial infarction-induced fixed perfusion deficits categorized by SRS score measured using QPS.**

<b>Variables</b>	<b>Mild (n=11)</b>	<b>Moderate (n=5)</b>	<b>Extreme (n=12)</b>
Age (years)	69±16	70 ± 9	64 ± 10
Diastolic volume (ml)	81 ± 30	107 ± 34	117 ± 44
Ejection fraction (%)	54 ± 6	46 ± 10	42 ± 11
SMS	18 ± 11	21 ± 8	33 ± 15
Stroke volume (ml)	38 ± 16	60 ± 30	70 ± 29

STS	11 ± 6	13 ± 5	20 ± 8
<p><i>*STS stands for the sum of left ventricular wall thickening, SMS for the sum of wall motility, and ± for standard deviation.</i></p>			

The predictive/discriminative variables, which were obtained via the Weka program (version 3.9.1, University of Waikato, New Zealand), consisted of 279 texture frames retrieved in the preceding stage. Examining a substantial quantity of textures obtained from each region of interest (ROI) is not feasible in a clinical setting. Therefore, it is essential to narrow down the dataset to identify the most valuable ones that effectively aid in classifying the D.F. from the myocardium with uniform uptake. To achieve this objective, the following actions were undertaken: 1) Utilizing Pearson correlation to decrease the number of texture frames, with values ranging from 0 to 85. Based on this criterion, a total of 50 out of 279 individuals (20%) were chosen (Arian et al., 2022).

Based on this criterion, 50/279 (20%) textures were chosen, and these textures were then classified using three models that are often used in the literature: 1) Random forest (R.F.), 2) LogitBoots (L.B.), and 3) AdaBoostm (A.B.), all utilizing ten-fold cross-validation. The models were contrasted using the area under the ROC curve (AUC), sensitivity, and specificity metrics (Ayx et al., 2023).

**STATISTICAL EVALUATION:**

The Jamovi program (Version 2.5.5.0, jamo-vi.org) was used to make it. The three figures that represent descriptive statistics are mean, deviation, and standard error. Plot square mean differences between segments with fixed defects and sections with homogeneous uptake were evaluated using the Student's t-test; a P value of less than 0.05 indicated statistical significance between the two groups. To determine each texture's sensitivity, specificity, and area under the ROC curve (AUC), a binomial linear regression analysis was carried out (Amini et al., 2023).

**RESULTS:**

The average age of the 28 patients in the population, 20 men and eight women was 67±11 years old, ranging from 44 to 93 years old. Fixed perfusion deficiencies (F.D.) with matching LV function were classified as mild (18%), moderate (39%), or severe (43%) based on polar maps and SRS summed score values (Table 1). The mean SRS for the 28 individuals was 12 ± 5. Based on the polar maps that Cendar-Sinai (MPCS) offered, the perfusion of D.F.'s vascular localization was found in 11 of the right coronary arteries (ACD20) and 17 of the anterior descending artery (ADA). With a sensitivity, specificity, and AUC of 100%, the R.F. and L.B. models were able to distinguish between D.F. structures and those that corresponded to homogenous uptake in the myocardium, whether or not the factors mentioned in Table 1 were included in the model (Zhang et al., 2022).

**TABLE 2: Characteristics of five texture tables comparing D.F. to myocardium with homogenous uptake, with significant values (p<0.05).**

Checked texture	Bunch	Ngeneo	Half	D.S.	ES	P
135dr_ShrtREmp	DF	28	43415	09.5	285.3	<0.001

	MCH	28	1452.0	411.6	77.79	
45dgr_ShrtrREmp	DF	28	861281	2.17e+6	409810.0	0.04
	MCH	28	329.4	164.0	30.99	
45dgr_Fraction	DF	28	414	74.5	14.1	<0.001
	MCH	28	55.1	13.5	2.56	
S(2,2)InvDfMom	DF	28	966	197.5	37.3	<0.001
	MCH	28	83.3	46.6	8.80	
Horzl_Fraction	DF	28	301	53.5	10.1	<0.001
	MCH	28	34.8	12.5	2.35	

*\*DF= fixed defects, MC= myocardium with homogeneous uptake, DS= standard deviation, ES= standard error*

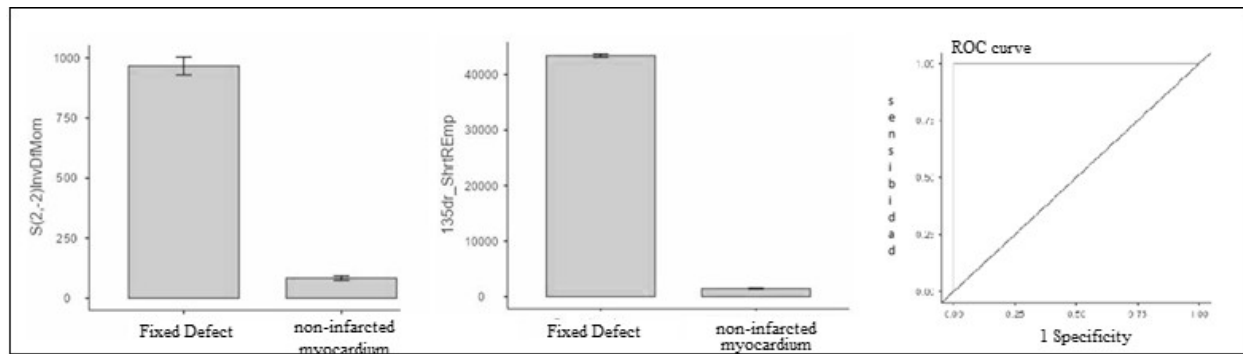


Figure 2 displays the difference between two of the top five radionics for repaired perfusion deficiencies resulting from fibrosis or scarring in non-infarcted myocardium. The area under the ROC curve (AUC) is 100%, demonstrating that radionics have a high degree of accuracy in differentiating between the two fabrics.

**Regression with binomials**

Student's T-test was used to compare the 50 variables chosen by the WEKA software using Pearson correlation and decrease the textures according to the significance of the differences between the variables. AUC = 92% ± 0.08, ranges 70%-100%, sensitivity; 90% ± 0.11, ranges 60%-100%; specificity; 75% ± 0.19, ranges 18%-100%). Twenty-five of the 50 (50%) had D.F. significantly higher than homogeneous uptake in the myocardium (p < 0.05). Structures were then compared using binomial linear regression, which revealed results in 22/25 (88%) statistically significant when I U.C. values were > 70%. To distinguish between myocardium with homogeneous MIBI uptake and D.F. caused by fibrosis or scarring, five out of 22 textures had AUC values of 100%, which is thought to be the best indicator of cardiomyocytes with intact sarcolemma and healthy mitochondria (Table 2, Figure 2) (Arian et al., 2022).

The chance of accurately classifying the highest positive parameter (heterogeneous tissue, the lowest negative) is what makes the ROC curve, which is frequently employed in pattern recognition research, helpful

in determining whether a feature or parameter is discriminative. Homogenous absorption in the myocardium), which is why it was thought that these five structures, either alone or in combination, were the most effective in identifying the existence of heterogeneity in the D.F. (Figure 2). Table 3 displays the quantification of textures concerning the magnitude of repaired perfusion faults (Table 1) (Xu et al., 2021).

**DISCUSSION:**

In routine practice, hypoperfusion at rest is visually interpreted as secondary to prior myocardial infarction, whose histopathological expression is fibrosis/scar, with heterogeneity in the infarcted myocardium, alteration not visible in images quantifiable via radionics texture. These patients have a clinical history of chronic myocardial infarction and are studied with PMSG with MIBI 99mTC. The ROI (region of interest) of pictures from CRMN, PET, SPECT, and other tests is measured by this tool. Even in the case of severe coronary heart disease, the myocardium can be detected and classified using artificial intelligence models based on differences in pixel intensity. This is done for myocardiums with various textures (such as scars, myocarditis, hypertrophic cardiomyopathy, etc.), including the one that is visualized with homogeneous MIBI (Cetin et al., 2020).

**TABLE 3: Radiomics in myocardial with capt and mild, moderate, and severe corrected perfusion deficits assessed by SRS with QPS**

Radiomic Texture Pictures	MCH	Mild	Moderate	Severe
135dr_ShrtREmp	1452 ± 411*	43586 ± 2176*	43204±1399 *	43264±1054 *
45dgr_ShrtREmp	329 ± 164*	3521 ± 938 *	1.1e+6 ± 2.6e+6*	480109 ±1.5e*6*
45dgr_Fraction	55 ± 13*	352 ± 58 *	438 ± 63 *	415 ± 85 *
S(2,2)InvDfMom	83 ± 46 *	1005 ± 147*	963 ± 241 *	945 ±1 85 *
Horzl_Fraction	35 ±12*	246 ± 68 *	324 ± 42 *	304 ± 43 *

\*MC= myocardium with homogeneous uptake, ± = Standard deviation, \* p<0.01

Using the Mazda program, the clinically interpreted areas (D.F., myocardial cardio with homogeneous uptake, radionics textures) were extracted from the ROIs drawn on the polar maps in this MIBI-gate SPECT myocardial perfusion study with 99mTc at rest. These areas were then classified using the artificial intelligence models RandomForest and LogitBoost and discriminated via logistic regression analysis (Figure 1). These initial findings imply that radiomic textures can be extracted from myocardial perfusion images using 99mTc-MIBI. Heterogeneity in F.D. can be detected using BMI as a means of classifying it as mild, moderate, or severe. These textures can then be distinguished from homogeneous capture textures using RF LB AI and binomial logistic regression with 100% AUC (Table 1). In contrast to myocardium with homogeneous uptake, the radiomic textures 135dr\_ShrtREmp, 45dgr\_ShrtREmp, 45dgr\_Fraction, S(2,-2)InvDf-Mom, and Horzl\_Fraction, which correspond to the co-occurrence matrix and run length, showed statistically significant differences in their ability to discriminate between D.F.s secondary to fibrosis/scar (Table 2-3) (Feng et al., 2022).

According to the author, several investigations using gadolinium-enhanced CRMN have shown the clinical value of radiomics in quantifying myocardial infarction-related scar heterogeneity. These five combined

or independent radiomic tables, shown in Table 2, quantify the heterogeneity in mild, moderate, or severe F.D. in PMSG images with MIBI 99mTc of patients with chronic myocardial infarction (Table 3). This is done by extrapolating these works and what has been published in the literature to the present results. These findings imply that the radiomics technique is characterizing the myocardial scar by detecting heterogeneity in F.D. This technique may help extend the size of the perfusion defect, as the quantification of the infarcted tissue mass (which is also included in the quantitative PMSG programs) may function as a stand-alone predictor of the risk of arrhythmic events (Badano et al., 2020).

This is the only study that we are aware of that uses radiomic textures in PMSG pictures of individuals who have had a persistent MI. It was not necessary to perform new myocardial perfusion SPECT acquisitions or give extra doses of 99mTc-MIBI to apply radionics.

A novel approach called "radiomics" is applied explicitly to cardiac imaging using CRMN. The radionics approach, which detects heterogeneity, could be employed in other cardiomyopathies (e.g., hypertrophic cardiomyopathy) as well as in other nuclear cardiology studies employing 99mTc-MIBI SPECT, 83RbPET, or 125 Iodine-MIBG, even though the current study was conducted in F.D. using BMI (Shad et al., 2020).

#### LIMITATION:

It is necessary to take certain restrictions into account. Because this is a single-centre study, further patient participation and multicenter research are needed to corroborate the findings. Radiomics quantification in PMSG images is difficult because of the possibility of calculating hypoabsorption as texture due to low-resolution SPECT images or attenuation (this study uses a gamma camera without attenuation correction, which can be corrected using hybrid equipment). These factors could lead to false positive interpretations, whether they are secondary to the mammary gland, diaphragm, obesity, or other factors (in this study, images were probably suppressed when acquired in the prone position) (Wang et al., 2023).

#### CONCLUSION:

Based on this initial experience, radiomics on myocardial perfusion pictures using 99mTc MIBI SPECT is feasible and may help identify heterogeneity in fixed perfusion deficits in patients with chronic myocardial infarction, independent of the extent of the defect. Prospective studies in the future will show whether adding radiomics to PMSG improves its diagnostic and predictive utility in patients with chronic myocardial infarction when compared to other quantitative markers.

#### REFERENCES:

- Amini, M., Pursamimi, M., Hajianfar, G., Salimi, Y., Saberi, A., Mehri-Kakavand, G., Nazari, M., Ghorbani, M., Shalhaf, A., & Shiri, I. (2023). Machine learning-based diagnosis and risk classification of coronary artery disease using myocardial perfusion imaging SPECT: A radiomics study. *Scientific reports*, 13(1), 14920.
- Arian, F., Amini, M., Mostafaei, S., Rezaei Kalantari, K., Haddadi Avval, A., Shahbazi, Z., Kasani, K., Bitarafan Rajabi, A., Chatterjee, S., & Oveisi, M. (2022). Myocardial function prediction after coronary artery bypass grafting using MRI radiomic features and machine learning algorithms. *Journal of digital imaging*, 35(6), 1708-1718.
- Ayx, I., Froelich, M. F., Baumann, S., Papavassiliu, T., & Schoenberg, S. O. (2023). Radiomics in cardiac computed tomography. *Diagnostics*, 13(2), 307.
- Badano, L. P., Keller, D. M., Muraru, D., Torlasco, C., & Parati, G. (2020). Artificial intelligence and cardiovascular imaging: A win-win combination. *Anatolian Journal of Cardiology/Anadolu Kardiyoloji Dergisi*, 24(4).
- Benfante, V., Stefano, A., Ali, M., Laudicella, R., Arancio, W., Cucchiara, A., Caruso, F., Cammarata, F. P., Coronello, C., & Russo, G. (2023). An Overview of In Vitro Assays of 64Cu-, 68Ga-, 125I-, and 99mTc-Labelled Radiopharmaceuticals Using Radiometric Counters in the Era of Radiotheranostics. *Diagnostics*, 13(7), 1210.

- Cetin, I., Raisi-Estabragh, Z., Petersen, S. E., Napel, S., Piechnik, S. K., Neubauer, S., Gonzalez Ballester, M. A., Camara, O., & Lekadir, K. (2020). Radiomics signatures of cardiovascular risk factors in cardiac MRI: results from the U.K. Biobank. *Frontiers in Cardiovascular Medicine*, 7, 591368.
- Feng, Y., Xu, Z., Zhang, L., Zhang, Y., Xu, H., Zhuang, X., Zhang, H., & Xie, X. (2022). Machine-learning-derived radionics signature of per coronary tissue in coronary C.T. angiography associated with functional ischemia. *Frontiers in physiology*, 13, 980996.
- Lin, A., & Dey, D. (2022). CT-based radiomics and machine learning for the prediction of myocardial ischemia: Toward increasing quantification. *Journal of Nuclear Cardiology*, 29(1), 275-277.
- Noguera, E., Castro, R., Molina, D., Sala, L. P., Freytes, A., & Yonni, C. (2022). Radiómica en infarto de miocardio crónico con 99MTC-MIBI SPECT. Primeras experiencias. *Revista de la Federación Argentina de Cardiología*, 51(4), 147-152.
- Rdzanek, A., Sygitowicz, G., Grabowski, M., & Tomaniak, M. An update on cardiovascular disorders in systemic lupus erythematosus.
- Shad, R., Quach, N., Fong, R., Langlotz, C. P., Kong, S., Kasinpila, P., Amsallem, M., Haddad, F., Shudo, Y., & Woo, Y. J. (2020). A radiomics approach to artificial intelligence in echocardiography: Predicting post-operative right ventricular failure. *medRxiv*, 2020.2005. 2005.20092494.
- Solanki, R., Sood, A., Debi, U., Singhal, M., Bahl, A., Dhooria, S., Singh, H., & Mehrotra, S. (2022). Category: Cardiology.
- Uz Zaman, M. (2022). ABSTRACTS-38th ANNUAL RSP CONFERENCE-KARACHI (25th-27th November 2022). *PJR*, 32(4).
- Wang, Z., Zhang, J., Zhang, A., Sun, Y., Su, M., You, H., Zhang, R., Jin, Q., Shi, J., & Zhao, D. (2023). The role of epicardial and pericoronary adipose tissue radiomics in identifying patients with non-ST-segment elevation myocardial infarction from unstable angina. *Heliyon*, 9(5).
- Xu, P., Xue, Y., Schoepf, U. J., Varga-Szemes, A., Griffith, J., Yacoub, B., Zhou, F., Zhou, C., Yang, Y., & Xing, W. (2021). Radiomics: the next frontier of cardiac computed tomography. *Circulation: Cardiovascular Imaging*, 14(3), e011747.
- Zhang, L., Xu, Z., Jiang, B., Zhang, Y., Wang, L., De Bock, G. H., Vliegenthart, R., & Xie, X. (2022). Machine-learning-based radiomics identifies atrial fibrillation on the epicardial fat in contrast-enhanced and non-enhanced chest C.T. *The British Journal of Radiology*, 95(1135), 20211274.
- Zhao, H., Yuan, L., Chen, Z., Liao, Y., & Lin, J. (2021). Exploring the diagnostic effectiveness for myocardial ischemia based on CCTA myocardial texture features. *BMC Cardiovascular Disorders*, 21(1), 416.